



Furfuryl alcohol from furfural hydrogenation over copper supported on SBA-15 silica catalysts



D. Vargas-Hernández^a, J.M. Rubio-Caballero^b, J. Santamaría-González^b, R. Moreno-Tost^b, J.M. Mérida-Robles^{b,*}, M.A. Pérez-Cruz^a, A. Jiménez-López^b, R. Hernández-Huesca^a, P. Maireles-Torres^b

^a Centro de Investigaciones de la Facultad de Ciencias Químicas de la Benemérita Universidad Autónoma de Puebla, Blvd. 14 Sur y Av. San Claudio Ciudad Universitaria, 72570 Puebla, Mexico

^b Departamento de Química Inorgánica, Cristalografía y Mineralogía (Unidad Asociada al ICP-CSIC), Facultad de Ciencias, Universidad de Málaga, Campus de Teatinos, 29071 Málaga, Spain

ARTICLE INFO

Article history:

Received 10 October 2013

Received in revised form

25 November 2013

Accepted 28 November 2013

Available online 6 December 2013

Keywords:

Cu-SBA-15

Furfural

Hydrogenation

Furfuryl alcohol

Copper

ABSTRACT

Vapor phase furfural hydrogenation has been investigated over Cu supported on SBA-15 silica catalysts. These SBA-Cu catalysts, with variable Cu loadings (8, 15 and 20 wt%), have been prepared by impregnation and characterized by N₂ sorption, XRD, XPS, N₂O decomposition and TEM techniques. Compared with copper chromite, SBA-Cu catalysts showed a better catalytic performance, reaching a furfural conversion of 54 mol% and a selectivity to furfuryl alcohol of 95 mol%, after 5 h of time-on-stream at 170 °C, with the 15 wt% Cu catalyst. The studies of the used catalysts by CNH analysis and thermo-programmed oxidation (TPO) evidenced a lower amount of carbonaceous deposits on this used SBA-15Cu catalyst. Moreover, the study of the copper dispersion by XPS, before and after the catalytic test, revealed that this intermediate copper loading gives rise to the most stable copper particles. The evaluation of the effect of different reaction parameters, such as reaction temperature (170–270 °C), catalyst loadings and furfural concentration and H₂ flow, on the catalytic performance has demonstrated that higher conversion are attained at low reaction temperature, and, as expected, by using high catalyst weight and low furfural feed.

© 2013 Elsevier B.V. All rights reserved.

1. Introduction

Humanity is facing the need of finding new energy sources, due to the increasing energy demand, growing environmental concerns and mainly the declining of petroleum reserves. In this sense, research attention is being paid to the exploration of new no-fossil carbon resources, in order to take advantage of the technology developed as well as obeying the more severe constraints about greenhouse gas emissions. The research regarding catalytic transformations of different biomass-derived compounds is currently very active. Lignocellulose is a potential sustainable and renewable organic carbon source. It also provides opportunities to secure the local supply energy when it is produced locally [1,2].

Furfural is a promising platform as a building block for fuels and chemicals. Furfural can be catalytically converted into 2-methyl furan or 2-methyl tetrahydrofuran, used in innovative P-series fuels, or ethyl levulinate, γ -valerolactone, ethyl furfuryl

ether, which are employed as biofuels or fuel additives. Thus, for instance, the potential of 2-methyl furan as biofuels has been corroborated by Lange et al. [2]. Furfural is usually obtained by acid-catalyzed dehydration of pentoses, a five carbon sugar, such as xylose and arabinose. Furfural is also produced by fast pyrolysis of biomass. However, the high oxygen content makes it unstable against condensation and polymerization reactions that provide furfural undesirable storage properties. Hydrogenation of furfural to furfuryl alcohol is a method used to avoid these undesired reactions [3].

The direct conversion of furfural into furfuryl alcohol, methylfuran and furan via metal-catalyzed hydrogenation, reduction and decarbonylation reactions, is a strategic and ultimate industrial source for the production of a wide range of derivatives. Thus, furfuryl amine, furoic acid, α -methylfurfuryl alcohol can be produced in one step from furfural. Other important fine chemicals derived from furfural are 2-acetyl furan, 2,5-dimethoxydihydrofuran and 5-dimethylaminomethylfurfuryl alcohol [2].

Furfuryl alcohol is an important chemical well known in polymer industry, mainly used for the production of thermostatic resins, liquid resins for strengthening ceramics, as well as in the

* Corresponding author. Tel.: +34 952132021; fax: +34 952131870.

E-mail address: jmerida@uma.es (J.M. Mérida-Robles).

production of various synthetic fibers, rubbers-resins and farm chemicals. Besides, as chemical intermediate, it is employed for the manufacture of lysine, vitamin C, lubricants, dispersing agents and plasticizers [4].

Furfuryl alcohol can be produced through hydrogenation of furfural, either in liquid or vapor phase. The vapor phase hydrogenation is usually preferred because it can be carried out at atmospheric pressure. However, in both cases, the main drawback is the low selectivity to furfuryl alcohol, where the catalyst can play a key role. Copper chromite has been used in the furan industry for the selective hydrogenation of furfural to furfuryl alcohol for decades [5]. However, its moderate activity and high toxicity, which causes severe environmental pollution, have increased the scientific interest for developing new Cr-free catalysts which exhibit high selectivity for furfuryl alcohol [6].

Hydrogenation of furfural in liquid phase has been widely studied, using supported metals and amorphous alloys as catalysts, mainly copper chromite, Cu, Ni, Mo, Co, Pt, Rh, Ru and Pd [3–5,7–14] and Ni-P, Ni-B and Ni-P-B Ultrafine Materials [15]. However, a second metal or promoter is added sometimes for improving the activity or/and the selectivity, by increasing the surface area or acting as Lewis acid site to polarize the C=O bond. Among them, systems based on Ni or Co modified with Mo [16], Ni-Fe, Cu-Ca bimetallic catalysts [11,17], promoters such as Co, Zn, Fe, Cr, Pd and Ni in Cu-MgO [18], Ce [19], Ni-Fe-B [20], or heteropolyacids have showed high selectivity (98%) to furfuryl alcohol and conversion close to 100%. Nevertheless, the main drawback is that most of them cannot be reused [21].

While hydrogenation of furfural in liquid phase requires high pressures, it is carried out under mild conditions in gas phase, reducing costs. In this sense, some works concerning hydrogenation of furfural to furfuryl alcohol in gas phase have been recently reported. Although different types of supports, such as MgO and SiO₂, have been used in order to increase the surface area and to enhance the metal-support interaction, Cu has been the most employed metal, due to its high activity and selectivity toward furfuryl alcohol [3,4,7,9,12,14,17,18]. However, an active catalyst to substitute copper chromite catalyst has not been developed yet, since most of them are unsuitable for industrial applications owing to severe deactivation phenomena.

The aim of this work is to investigate the furfural catalytic hydrogenation in vapor phase over mesoporous silica-supported Cu catalysts. The catalytic behavior of these environmentally friendly materials was compared with that of a copper chromite. The effect of different experimental parameters, such as catalyst loading, reaction temperature, weight of catalyst and furfural feed, on the catalytic performance was studied.

2. Experimental

2.1. Catalyst synthesis and characterization

The synthesis of SBA-15 silica was carried out as reported by Zhao et al. [22]. The SBA-Cu catalysts were prepared by incipient wetness impregnation with aqueous solutions of Cu(NO₃)₂·3H₂O (Aldrich, >99% purity). After impregnation, catalysts were dried overnight at room temperature, and finally calcined for 6 h at 400 °C, with a heating rate of 1 °C/min. The metal loading ranges between 8 and 20 wt% of Cu. The catalysts were labeled as SBA-xCu, where x is the wt% of Cu. For comparison, a commercial copper chromite (Cu-Cr) was also studied (CuCr₂O₄·CuO, Aldrich).

Elemental analysis was performed on a PERKIN-ELMER 2400 CHN with a LECO VTF900 pyrolysis oven. Cu contents have been determined by atomic adsorption spectroscopy (AAS) by using a Varian SPECTRAA 50.

Powder X-ray diffraction (XRD) patterns were obtained by using a Siemens D5000 automated diffractometer, over a 2θ range with Bragg–Brentano geometry using the Cu Kα radiation and a graphite monochromator.

The morphology of catalysts was evaluated by Transmission Electron Microscopy (TEM). Before TEM analysis, samples were reduced *ex situ* in pure H₂ (60 ml/min) at 350 °C for 2 h, and stored in cyclohexane (Sigma-Aldrich, 99% purity).

X-ray photoelectron spectroscopy (XPS) studies were performed with a Physical Electronics PHI 5700 spectrometer equipped with a hemispherical electron analyzer (model 80-365B) and a Mg Kα (1253.6 eV) X-ray source. High-resolution spectra were recorded at 45° take-off angle by a concentric hemispherical analyzer operating in the constant pass energy mode at 29.35 eV, using a 720 μm diameter analysis area. Charge referencing was done against adventitious carbon (C 1s at 284.8 eV). The pressure in the analysis chamber was kept lower than 5 × 10⁻⁶ Pa. PHI ACCESS ESCA-V6.0 F software package was used for data acquisition and analysis. A Shirley-type background was subtracted from the signals. Recorded spectra were always fitted using Gauss–Lorentz curves in order to determinate more accurately the binding energy of the different element core levels. The samples underwent the same aforementioned *ex situ* treatment before XPS analysis.

N₂ adsorption–desorption isotherms at –196 °C of calcined catalysts were obtained using an ASAP 2020 model of gas adsorption analyzer from Micromeritics, Inc. Prior N₂ adsorption, samples were evacuated overnight at 200 °C and 1 × 10⁻² Pa. Pore size distributions were calculated with the BJH method [23].

The reducibility of the calcined samples was determined by H₂ temperature-programmed reduction (H₂-TPR). For these measurements, 80 mg of sample was placed in a quartz reactor and heated at 100 °C under a He flow of 35 ml/min, and held at this temperature for 1 h. The reactor was then cooled down to 50 °C and the sample exposed to a stream of 47 ml/min of 10% H₂/Ar. Subsequently, the sample was heated up to 700 °C at a heating rate of 10 °C/min. The amount of hydrogen consumed as a function of temperature was monitored on-line on a TCD detector. The water formed during reduction was collected with a cryogenic trap at –85 °C before chromatographic analysis.

Copper surface area and dispersion were calculated by N₂O decomposition method. This method is based on the formation of a monolayer of Cu₂O by oxidation of Cu⁰ with a N₂O flow, according to the reaction: 2Cu⁰ + N₂O → Cu₂O + N₂. Before analysis, the CuO phase is reduced with a flow mixture of 10 vol.% H₂/Ar at 5 °C/min at 350 °C. Then, the catalyst is purged under He and cooled down to 60 °C. The oxidation of Cu⁰ to Cu⁺ is carried out by chemisorption of N₂O (5 vol.% N₂O/He) at 60 °C during 1 h. Then, the catalyst was again purged with an Ar flow and cooled to room temperature. After this, a temperature programmed reduction was carried out similarly to TPR, raising the temperature up to 350 °C on the freshly oxidized Cu₂O surface in order to reduce Cu₂O to Cu.

Temperature-programmed oxidation analyses (TPO) were performed in a METTLER TOLEDO TGA/DSC 1 apparatus equipped with a HT1600 furnace and a MX5 balance with a DSC HSS2 Pt-Rh sensor. Temperature was varied from 30 to 400 °C at a rate of 5 °C/min, under an O₂ flow of 50 ml/min.

2.2. Catalytic activity

The vapor-phase reduction of furfural was conducted in a ¼" tubular quartz reactor. The pelletized catalyst (325–400 μm) was placed at the center of the reactor tube between two layers of glass beads and quartz wool. Catalysts were reduced *in situ* under a H₂ flow (60 ml/min, Airgas, 99.99%) for 2 h at 350 °C, prior to the catalytic test. After reduction, the catalysts were cooled down to the selected reaction temperature under a H₂ flow

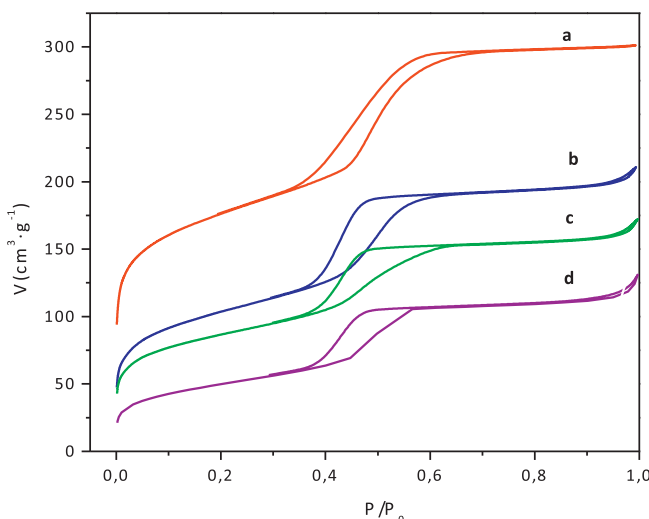


Fig. 1. N_2 adsorption–desorption isotherms: (a) SBA-15, (b) SBA-8Cu, (c) SBA-15Cu and (d) SBA-20Cu catalysts.

(10 ml/min). When the temperature was reached, a flow of furfural (Sigma–Aldrich) solution in cyclopentyl methyl ether (CPME) (Sigma–Aldrich) (5 vol.%) was continuously injected by using a HPLC pump. CPME is an environmentally friendly solvent that has been used in different organic reactions, thus, for instance, demonstrating to be a green co-solvent for the selective dehydration of lignocellulosic pentoses to furfural [24].

The reaction products were analyzed by gas chromatography (Agilent model 14A) with a Flame Ionization Detector. The product yield and selectivity were calculated and defined as follows:

$$\text{Conversion (\%)} = \frac{\text{mol of furfural converted}}{\text{mol of furfural fed}} \times 100$$

$$\text{Selectivity (\%)} = \frac{\text{mol of the product}}{\text{mol of furfural converted}} \times 100$$

3. Results and discussion

3.1. Characterization of copper catalysts

The Cu contents of the different catalysts, as determined by AAS, are displayed in Table 1. Thus, the Cu content of the synthesized SBA-xCu catalysts varies between 7.8 and 20.2 wt%, while for the Cu-Cr sample was much higher (39.6 wt%).

N_2 adsorption–desorption isotherms for SBA-15 and calcined SBA-xCu are presented in Fig. 1. All of them exhibited a Type-IV isotherm according to the IUPAC classification, with a H1 hysteresis loop. The shape of the isotherm of pure SBA-15 was preserved even for the catalyst with the highest copper content, which means that, after the impregnation and subsequent calcination of copper precursors, the mesoporous nature of the solid was maintained. The evaluation of the textural properties of calcined samples from nitrogen adsorption–desorption isotherms at -196°C reveals that the BET surface area decreases progressively with the loading of copper, with a drastic reduction for the material with the highest Cu content (SBA-20Cu) (Table 1). However, excepting for the latter sample, the average pore diameters barely change in comparison with the mesoporous silica, used as support, thus pointing to the presence of copper oxide particles blocking partially the entrance to the mesoporous framework.

The low-angle powder XRD patterns of the SBA-15 support and SBA-xCu catalysts (Fig. 2) exhibit a well-resolved diffraction peak, which can be indexed in a hexagonal unit cell as corresponding to

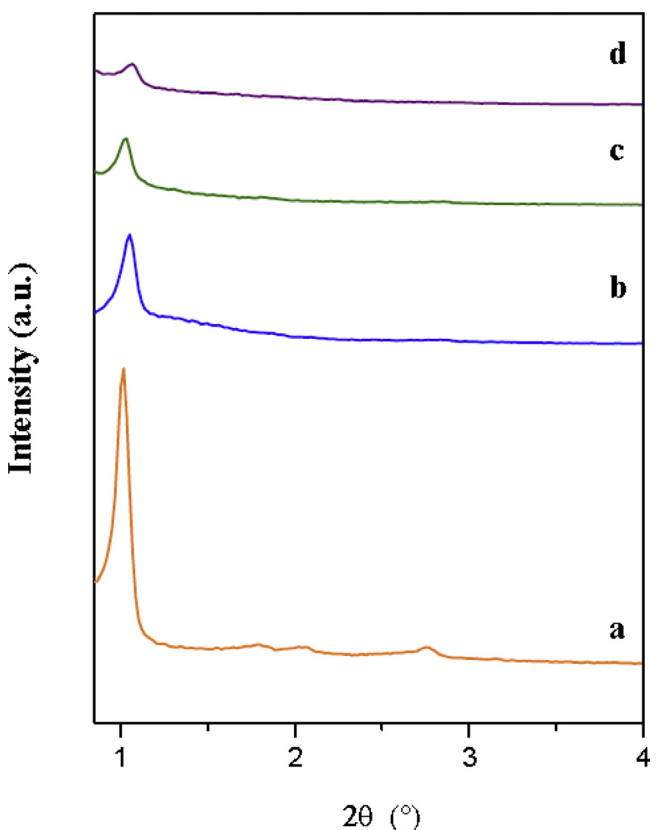


Fig. 2. Low angle XRD patterns of (a) SBA-15, (b) SBA-8Cu, (c) SBA-15Cu, (d) SBA-20Cu catalysts.

the (100) reflection of the SBA-15 silica, confirming that the mesoporous structure is preserved after copper incorporation. However, the presence of copper on the support gives rise to a decrease in the intensity of this low angle peak, which can be explained by the scattering effect of the metallic copper particles.

The presence of metallic copper (Cu^0) on the surface of catalysts, fresh (reduced) and spent (after reaction), can be deduced from XRD (Fig. 3). Thus, the characteristic diffraction lines of Cu^0 (fcc structure) are clearly visible at $2\theta (\text{°}) = 43.4$ and 50.5 (JCPDS 04-0836), excepting for the catalyst with the smallest amount of Cu (SBA-8Cu), and their intensities, as expected, increase with the copper loading. However, after reaction, copper chromite also shows the presence of weak peaks at $2\theta (\text{°}) = 31.4, 36.5$ and 62.4 , which point to the formation of CuCrO_2 crystallites (JCPDS-39-0247). These results suggest that the metallic copper in copper chromite is oxidized to Cu^+ , which reacts with Cr_2O_3 to form CuCrO_2 . This behavior of copper chromite, after reduction, has been already observed by Deutsch and Shanks in the study of the active species derived from Cu-chromite in C–O hydrogenolysis of furfuryl alcohol [25].

It is well known that reducibility of copper species depends on the preparation method, the nature of the support and precursor, as well as the experimental conditions used for the reduction step. Fig. 4 shows the TPR profiles of the calcined SBA-xCu catalysts and Cu-chromite. The quantification of H_2 consumption confirms the complete reduction of CuO to $\text{Cu}(0)$ at the temperature of 350°C . The existence of several defined ranges of hydrogen consumption in TPR profiles points to the presence of different Cu^{2+} species in calcined precursors. Two broad H_2 consumption bands of different intensity can be observed in the H_2 -TPR spectra of the supported copper catalysts, which can be assigned to the reduction of Cu^{2+} to Cu^0 . According to the literature [26], the low temperature band could be associated to the presence of finely dispersed CuO particles

Table 1

Physicochemical characterization of SBA-xCu and Cu-Cr catalysts.

Catalyst	Cu loading (wt%)	S_{BET} ($\text{m}^2 \text{ g}^{-1}$)	d_p (nm)	V_p ($\text{cm}^3 \text{ g}^{-1}$)	D_M (%)	S_M ($\text{m}^2 \text{ g}^{-1}$)	d_M (nm)
SBA-15	–	581	3.6	0.465	–	–	–
SBA-8Cu	7.8	369	3.9	0.326	58.0	389.3	1.7
SBA-15Cu	14.1	307	4.0	0.267	38.5	260.4	2.6
SBA-20Cu	20.2	179	4.3	0.202	9.7	65.8	10.3
Cu-Cr	39.6	46	18.0	0.217	24.5	165.8	4.1

and the second one to larger particles of bulk CuO. These findings are in agreement with the XRD data of reduced catalysts, where the presence of diffraction peaks associated to metallic copper is not detected in the SBA-8Cu catalyst. With the increase of Cu loading, the relative intensity of the hydrogen consumption peaks change gradually, by increasing the second one which could be explained by the formation of large copper oxide particles. This agrees with previous studies, where the presence of two reduction peaks in the H_2 -TPR curves of Cu/SiO₂ and co-precipitated Cu-MgO catalysts have been shown [3,10]. On the other hand, copper(II) in Cu-chromite is fully reduced at temperatures lower than 250 °C.

Therefore, it could be inferred from the TPR profiles that complete reduction of copper in this series of catalysts can be expected after a reduction treatment at 350 °C.

Regarding the copper dispersion, the results of the titration with N₂O at 60 °C are presented in Table 1. The SBA-xCu catalysts showed high dispersion (D_M) and metal area (S_M) values that decreased with Cu content. It was possible to estimate the average particle size (d_M) assuming cubic metal particles and using a surface density of Cu atoms of 1.08×10^{15} at cm^{-2} . Thus, the estimated values range between 1.7 and 10.3 nm, indicating that small metal copper particles are formed by reduction of the samples with the highly dispersed CuO phases present on the SBA surface, as previously showed by XRD patterns. As expected, the average particle sizes increase with the copper loading.

Catalysts have been characterized by X-ray photoelectron spectroscopy to obtain more information about the Cu oxidation state and the chemical composition of the catalyst surface. The binding energy values of Cu 2p_{3/2}, O 1s and Si 2p along with the Si/Cu atomic ratios, of both fresh and spent catalysts, are presented in Table 2. The Si 2p binding energy (BE) value, in all the SBA-xCu catalysts, is very similar, and the average value of 103.5 eV is typical of silica. The O 1s signal is symmetrical and appears at 533 eV in the SBA-xCu catalysts, lowering until 530 eV in copper chromite. These BE values for O 1s are characteristics of silica and metal oxide, respectively. The Cu 2p_{3/2} signal at 932–933 eV is due to the presence of metallic copper and/or Cu(I) species, whereas surface copper(II) species are not detected, as confirmed by the absence of XPS signals at 934–935 eV and the typical shake-up satellite at 940–945 eV, related with unoccupied 3d states (Fig. 5). However, the presence of Cu(II) is observed in the reduced copper chromite. For that reason, the Cu LMM kinetic energy of the Auger spectra has been used to distinguish between Cu(I) and Cu(0) (Fig. 6). In all cases, a broad band is observed with maxima at ca. 919 and 917 eV, which can be assigned to the contributions of Cu(0) and Cu(I), respectively [27].

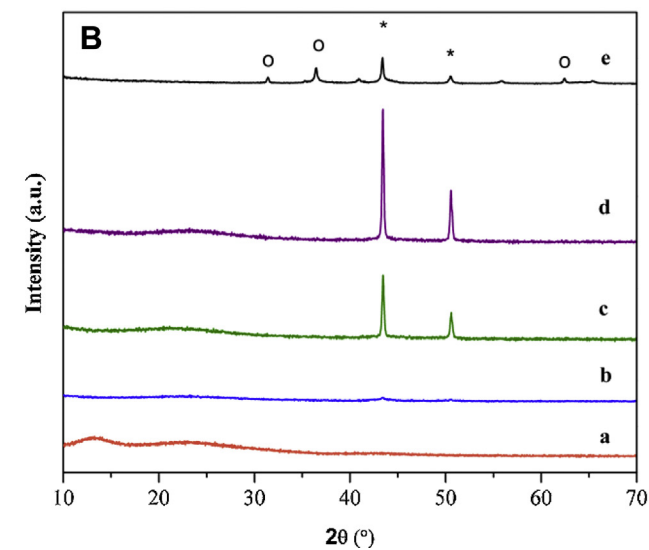
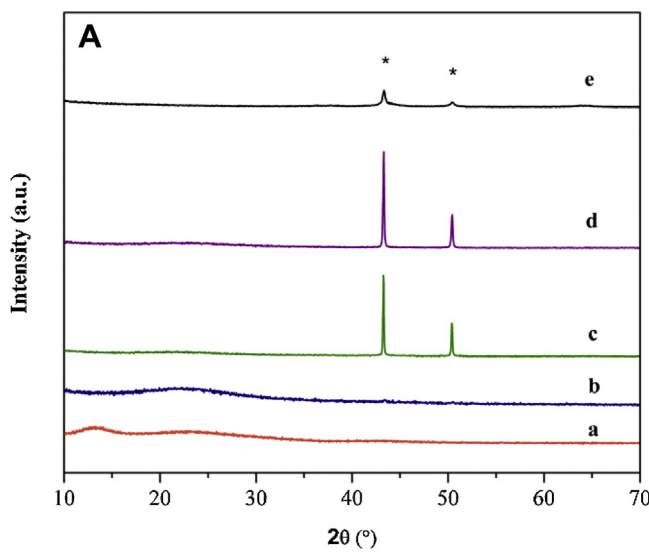


Fig. 3. XRD patterns for fresh (A) and used (B) catalysts: (a) SBA-15, (b) SBA-8Cu, (c) SBA-15Cu (d) SBA-20Cu and (e) Cu-Cr. The following phases are denoted: Cu⁰(*) and CuCrO₂(o).

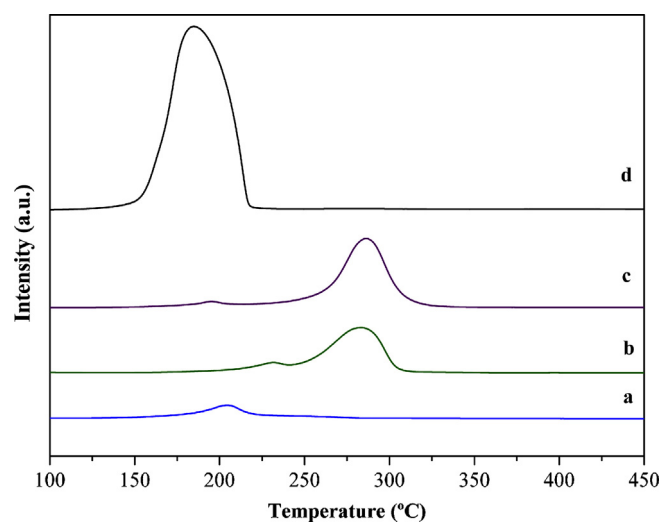


Fig. 4. Temperature programmed reduction profiles (TPR) of (a) SBA-8Cu, (b) SBA-15Cu, (c) SBA-20Cu and (d) Cu-Cr catalysts.

Table 2
XPS data of SBA-xCu and Cu-Cr catalysts.

Catalyst	Binding energy (eV)			Atomic ratio		
	Si 2p	O 1s	Cu 2p _{3/2}	Si(Cr)/Cu (fresh)	Si(Cr)/Cu (spent)	Si(Cr)/Cu (theor)
SBA-8Cu	103.6	533.1	933.2	53.3	32.1	12.5
SBA-15Cu	103.4	532.9	932.2	30.4	29.4	6.4
SBA-20Cu	103.5	533.0	932.0	13.1	20.8	4.2
Cu-Cr	—	530.2	932.5	2.66	2.79	1.0

In general, the Cu LMM bands shift to lower kinetic energy values after the catalytic reaction, thus evidencing the partial oxidation of Cu(0) to Cu(I), which has been proposed by some authors as the active sites for hydrogenation of furfural to furfuryl alcohol [12,13].

Concerning the surface Si/Cu atomic ratios, their values are always higher than the theoretical bulk ratios determined by ICP-AES, and they decrease, as expected, with the copper loading. This difference can be explained by considering not only the presence of copper particles into the mesoporous channels but also the existence of large copper particles on the external surface of the mesoporous support, as inferred from the presence of narrow diffraction peaks in the corresponding XRD patterns.

The TEM studies corroborate the results obtained by XRD and H₂-TPR analysis. The TEM micrographs of the SBA-8Cu and chromite catalysts, fresh and spent, are presented in Fig. 7. It can be observed that the metallic copper clusters are well dispersed on the silica support after reduction at 350 °C. As the copper loading increases, a more heterogeneous distribution of particles sizes is observed; thus, some metal particles of 35 nm are detected on the catalysts with the highest copper loading. In the case of the Cu-Cr catalyst, agglomerates of copper particles can be distinguished in the corresponding micrographs.

3.2. Catalytic activity studies

This series of copper-based catalysts has been tested in the vapor phase hydrogenation of furfural (FAL), at atmospheric pressure. Previously, the stability of the cyclopentyl methyl ether, used as solvent of furfural, was studied by feeding it into the reactor at 170 °C, in the presence of the SBA-15Cu catalyst. The results indicate that the solvent is stable, since it was fully recovered after 5 h of reaction time, without the presence of any new chemical compound. The results of catalytic activity as a function of time on stream (TOS), at 170 °C, reveal a strong deactivation (Fig. 8), which is more pronounced in the case of copper chromite. Thus, after 5 h of TOS,

copper chromite becomes almost inactive, whereas the supported catalyst with 15 wt% of copper loading still maintains a conversion higher than 50%. Hydrogenation of furfural can lead to different products, including furfuryl alcohol, 2-methylfuran, tetrahydrofurfuryl alcohol and other ring-opening products, depending on the catalysts employed and the reaction conditions. In this work, furfuryl alcohol (FOL) was obtained as the main product along with 2-methylfuran (MF) (Fig. 9). These results are in agreement with previous reports of furfural conversion over Cu-based catalysts, which show that furfuryl alcohol is the main product [4,6,11,14,18]. Sitthisa et al. [3] found that the conversion of furfural on Cu catalyst involves the interaction of the surface preferentially with the carbonyl group, rather than the furanic ring. Thus, DFT calculations have given evidence for a strong repulsion between the surface Cu (1 1 1) and the furan ring, presumably due to the overlap of the 3d band of Cu atoms and the anti-bonding orbital of the aromatic furan ring [3,28].

All the catalysts exhibit high selectivity toward FOL, which is the highest for a Cu content of 15 wt%. Nagaraja et al. have proposed that the presence of more Cu⁰, or less CuO species, gives rise to

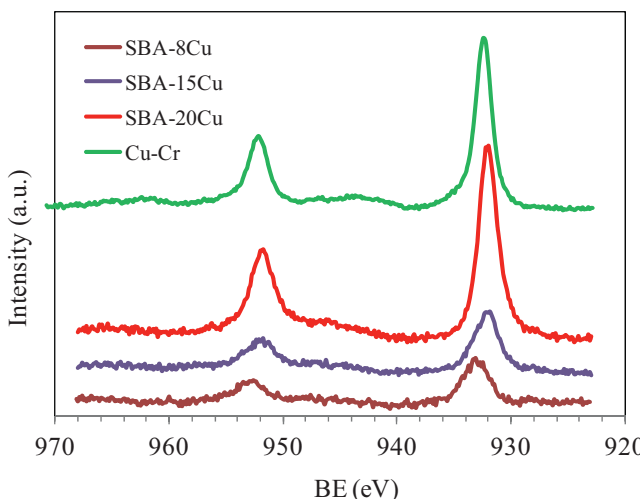


Fig. 5. XPS spectra in the Cu 2p region of reduced copper catalysts.

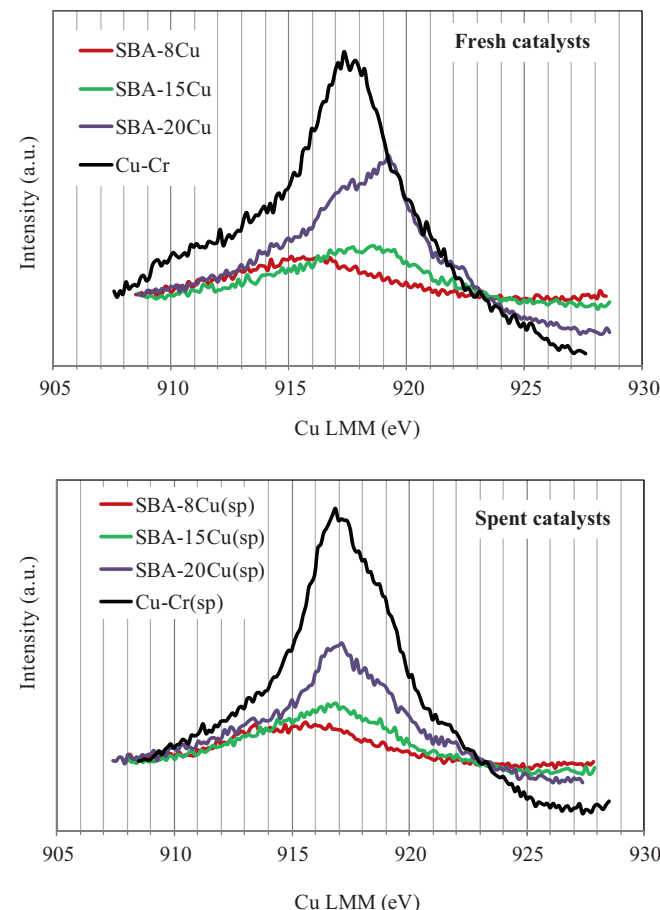


Fig. 6. Cu LMM Auger spectra of fresh and spent (sp) copper catalysts.

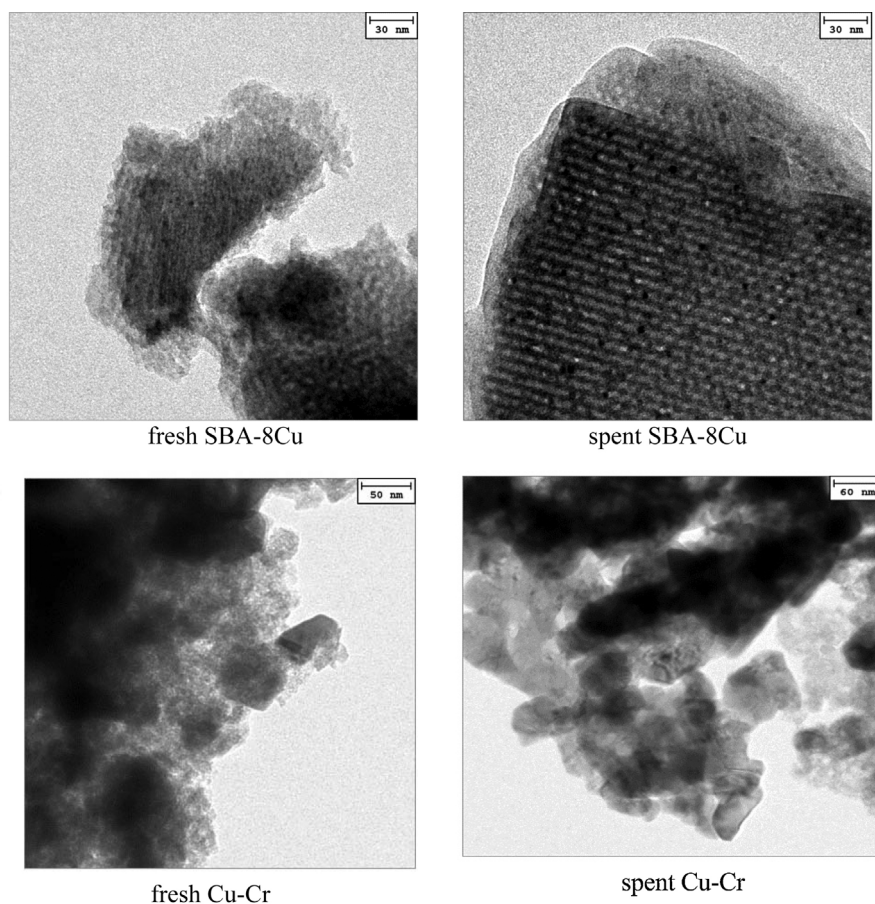


Fig. 7. TEM micrographs of the SBA-8Cu and Cr-Cu catalysts, before and after catalytic reaction.

a high catalytic activity toward the selective formation of FOL by hydrogenation of FAL [14]. A simple bimolecular surface reaction as a rate-determining step by correlating Cu^+ sites with activity and they proposed that the presence of both Cu^+ and Cu^0 species are required for optimum performance [4,13]. However, lack of required number of smaller Cu particles could make the SBA-20Cu catalyst less active in furfural hydrogenation, where the agglomeration of copper particles, as inferred from the surface Si/Cu molar ratio of the spent catalyst, could be responsible for its low activity compared to that of SBA-15Cu.

The deactivation process could be explained by the active copper site coverage by coke or adsorbed reactants/products, as revealed the high carbon percentages found in the spent catalysts by CHN analysis (Table 6), rather than the copper particle sintering or loss of the active Cu^+ species by reduction. The carbon deposition is the lowest for the SBA-15Cu material, which is that with the highest conversion values with TOS (Fig. 8). By comparing the Cu LMM spectra of fresh and used catalysts, it can be inferred that the amount of Cu^+ is more important after reaction, and the XPS results confirm that the existence of sintering could only be suggested for the

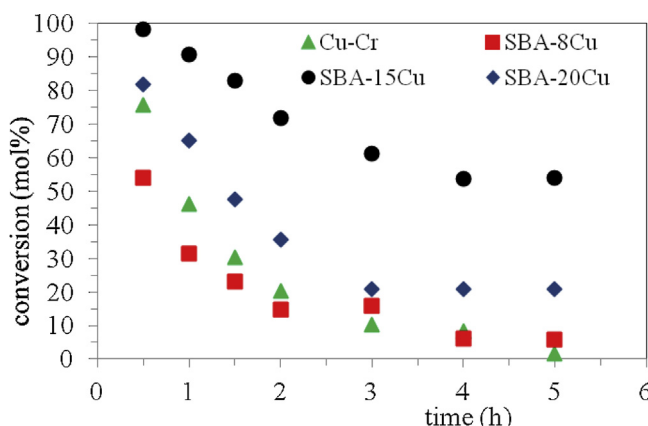


Fig. 8. Conversion of furfural over copper catalysts, at 170 °C, as a function of stream. Reaction conditions: $m_{\text{cat}} = 150 \text{ mg}$, H_2 flow = 10 ml/min, feed flow = 2.3 mmol/h.

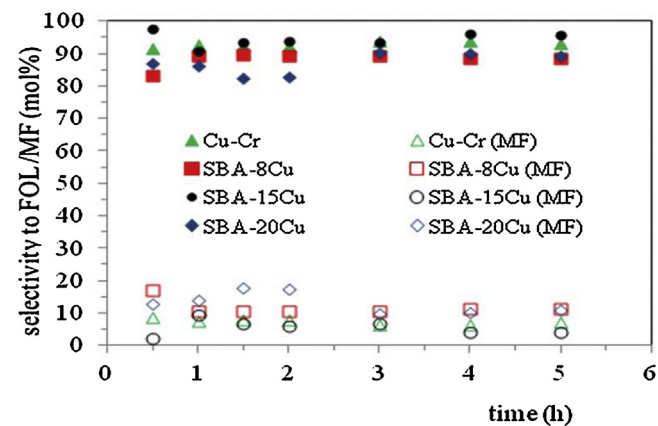


Fig. 9. Selectivity toward furfuryl alcohol and 2-methyl furan (MF) over copper catalysts, at 170 °C, as a function of time on stream. Reaction conditions: $m_{\text{cat}} = 150 \text{ mg}$, H_2 flow = 10 ml/min, feed flow = 2.3 mmol/h.

Table 3

Influence of the reaction temperature on the furfural hydrogenation over the SBA-15Cu catalyst (experimental conditions: $m_{\text{cat}} = 150 \text{ mg}$, H_2 flow = 10 ml/min, feed flow = 2.3 mmol/h, $t = 1 \text{ h}$).

$T (\text{ }^{\circ}\text{C})$	Conversion (%)	Selectivity (%)		Yield (%)	
		FOL	MF	FOL	MF
170	91.5	93.1	6.9	85.4	6.4
190	84.4	85.1	14.9	72.0	12.6
210	81.2	73.0	27.0	59.4	21.9
230	82.7	58.9	41.1	48.8	34.0
250	77.8	52.1	47.9	40.6	37.2
270	66.5	43.5	56.5	28.9	37.5

Table 4

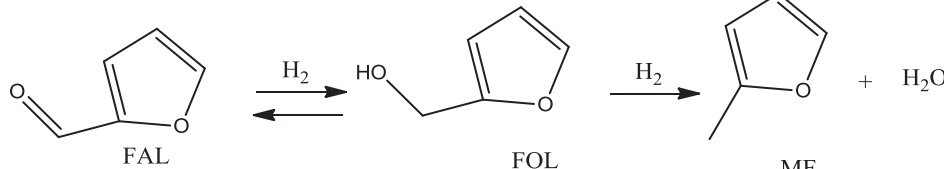
Influence of the catalyst weight on furfural hydrogenation over the SBA-15Cu catalyst (experimental conditions: $T = 170 \text{ }^{\circ}\text{C}$, H_2 flow = 10 ml/min, feed flow = 2.3 mmol/h, $t = 5 \text{ h}$).

Catalyst weight (mg)	Conversion (%)	Selectivity (%)		Yield (%)	
		FOL	MF	FOL	MF
100	33.9	82.4	17.6	27.9	5.9
150	54.1	95.8	4.2	51.8	2.3
200	69.4	89.5	10.5	62.0	7.3

catalyst with the highest copper loading (SBA-20Cu). It is noteworthy that the best catalytic performance is achieved for an intermediate copper loading, which is the catalyst that maintained the atomic Si/Cu ratio unchanged. A similar evolution of the catalytic activity as a function of the Cu loading in the FAL hydrogenation reaction has been observed by using Cu-MgO catalysts [4].

In the case of copper chromite, although the presence of carbonaceous deposits is detected, its strong deactivation could be also due to the formation of a CuCrO_2 phase from Cr_2O_3 and Cu^{+} , as evidenced the XRD pattern of the spent copper chromite (Fig. 3). This fact has been previously observed by Liu et al. in their work devoted to the study of the deactivation mechanism of this copper chromite for the same catalytic reaction at $200 \text{ }^{\circ}\text{C}$, where the coverage of Cu sites by this CuCrO_2 phase is proposed as an additional cause of catalyst deactivation [29].

On the other hand, the study of the influence of the reaction temperature, in the range 170 – $270 \text{ }^{\circ}\text{C}$ (Table 3), on conversion and product distribution over SBA-15Cu reveals a clear decrease in conversion as temperature rises, whereas MF production increases in detriment of FOL. Liu et al. [29] have reported the same behavior for copper chromite catalysts and the conversion decrease is attributed to the polymerization and adsorption of FOL molecules on the catalyst surface, which is favored at high temperatures. Therefore, it is apparent that furfural is first converted into FOL, which subsequent deoxygenation leads to MF, a reaction pathway previously proposed by Sitthisa et al. [3]:



Therefore, the lowest temperature, $170 \text{ }^{\circ}\text{C}$, was chosen to optimize other reaction parameters. The study of the catalytic behavior at lower temperatures was not possible due to the boiling point of furfural ($161.7 \text{ }^{\circ}\text{C}$).

Regarding the influence of the catalyst weight, the FAL conversion is ameliorated by increasing the amount of catalyst (Table 4). However, although conversion is improved, a higher amount of catalyst does not allow reaching much better FOL yield.

Table 5

Influence of the furfural feed on FAL hydrogenation over SBA-15Cu (experimental conditions: $m = 150 \text{ mg}$, $T = 170 \text{ }^{\circ}\text{C}$, H_2 flow = 10 ml/min, $t = 5 \text{ h}$).

Furfural feed (mmol/h)	Conversion (%)	Selectivity (%)		Yield (%)	
		FOL	MF	FOL	MF
1.6	58.3	84.8	15.2	49.5	8.9
2.3	54.1	95.8	4.2	51.8	2.3
3.4	31.9	91.0	9.0	29.0	2.9

Table 6

Data of TOF (reaction conditions: $m_{\text{cat}} = 150 \text{ mg}$, H_2 flow = 10 ml/min, feed flow = 2.3 mmol/h, $t = 5 \text{ h}$) and C analysis for the used SBA-xCu and Cu-Cr catalysts.

Catalyst	C (%)	TOF _{t=0} (FAL molecules converted s ⁻¹ Cu(0) ⁻¹)	
		FOL	MF
SBA-8Cu	10.3	2.66×10^{-3}	
SBA-15Cu	6.3	2.03×10^{-3}	
SBA-20Cu	9.7	1.32×10^{-3}	
Cu-Cr	4.8	0.72×10^{-3}	

Taking into account the differences in Cu dispersion and loading among the catalysts, it has been estimated initial TOF values in order to compare the intrinsic activity of the Cu metal sites. Table 6 shows the turnover frequency (TOF, s^{-1}) values, defined as molecules of FAL converted per second and Cu^0 site, calculated by extrapolation at zero time. From this study it is clear that TOF value is higher in SBA-xCu catalysts than in the Cu-Cr one. The highest TOF value was obtained for SBA-8Cu material, which showed a strong deactivation that can be associated to the deposition of coke and/or adsorbed reactants/products, as inferred from the highest C content found by CNH analysis in the spent catalyst. The SBA-20Cu catalyst exhibited the lowest TOF value of this series of supported copper catalysts, which could be due to a partial sintering of Cu^0 particles as evidenced the increase of the Si/Cu atomic ratio, obtained by XPS analysis, of the spent catalyst. Thus, the SBA-15Cu catalyst seems to be that with the appropriated loading and dispersion of Cu^0 to produce the highest conversion and FOL selectivity with TOS, with less deactivation, neither by C deposition nor metal sintering.

Finally, by feeding low FAL flows, a higher initial conversion is attained and the catalyst is more resistant to deactivation (Table 5). However, it is observed a decrease in FOL selectivity, favoring the formation of MF, thus resulting that a high feed of furfural inhibits MF production.

4. Conclusions

A series of supported copper catalysts has been prepared by impregnation and subsequent calcination of mesoporous SBA-15 silica with different loading of copper nitrate. The study of the

furfural hydrogenation over SBA-xCu and Cu-Cr catalysts indicated that all of them are active, and that the presence of Cu^0 – Cu^{+} species on the catalyst surface is responsible for the high activity and selectivity toward furfuryl alcohol. The SBA-15Cu catalyst shows the highest activity and selectivity toward the desired product at $170 \text{ }^{\circ}\text{C}$, when a H_2 flow 10 ml/min, 150 mg of catalyst and a furfural feed flow of 0.1875 ml/h were employed.

All catalysts undergo deactivation with time on stream, being more drastic for copper chromite. In the case of SBA- x Cu, the studies of the used catalysts by CNH analysis and thermo-programmed oxidation (TPO) evidenced the presence of carbonaceous deposits, which are lower for the used SBA-15Cu catalyst. Moreover, the study of the copper dispersion by XPS, before and after the catalytic test, revealed that this intermediate copper loading gives rise to the most stable copper particles.

Acknowledgments

The authors are grateful to financial support from Spanish Ministry of Economy and Competitiveness (CTQ2012-38204-C03-02), FEDER funds and Junta de Andalucía (P09-FQM-5070). RMT for the financial support under the Program Ramón y Cajal (RYC-2008-03387) and Consejo Nacional de Ciencia y Tecnología (CONACyT, México) for financial support via scholarships (219821).

References

- [1] L. Faba, E. Díaz, S. Ordóñez, *Catal. Today* 164 (2011) 451–456.
- [2] J.P. Lange, E. van der Heide, J. van der Buijtenen, R. Price, *ChemSusChem* 5 (2012) 150–166.
- [3] S. Sitthisa, T. Sooknoi, Y. Ma, P.B. Balbuena, D.E. Resasco, *J. Catal.* 277 (2011) 1–13.
- [4] B.M. Nagaraja, A.H. Padmasri, B. David Raju, K.S. Rama Rao, *J. Mol. Catal. A* 265 (2007) 90–97.
- [5] J. Kijenski, P. Winiarek, T. Paryjczak, A. Lewicki, A. Mikołajska, *Appl. Catal. A* 233 (2002) 171–182.
- [6] L. Baijun, L. Lianhai, W.B. Bingchun, C. Tianxi, K. Iwatani, *Appl. Catal. A* 171 (1998) 117–122.
- [7] S. Sitthisa, D.E. Resasco, *Catal. Lett.* 141 (2011) 784–791.
- [8] V. Vetere, A.B. Merlo, J.F. Ruggera, M.L. Casella, *J. Braz. Chem. Soc.* 21 (2010) 914–920.
- [9] W. Huang, H. Li, B. Zhu, Y. Feng, S. Wang, S. Zhang, *Ultrason. Sonochem.* 14 (2007) 67–74.
- [10] B.M. Nagaraja, V. Siva Kumar, V. Shasikala, A.H. Padmasri, B. Sreedhar, B. David Raju, K.S. Rama Rao, *Catal. Commun.* 4 (2003) 287–293.
- [11] X. Chen, H. Li, H. Luo, M. Qiao, *Appl. Catal. A* 233 (2002) 13–20.
- [12] R.S. Rao, R.T. Baker, M.A. Vannice, *Catal. Lett.* 60 (1999) 51–57.
- [13] R.S. Rao, R.T. Baker, M.A. Vannice, *J. Catal.* 171 (1997) 406–419.
- [14] B.M. Nagaraja, A.H. Padmasri, P. Seetharamulu, K. Hari Prasad Reddy, B. David Raju, K.S. Rama Rao, *J. Mol. Catal. A* 278 (2007) 29–37.
- [15] S.P. Lee, Y.W. Chen, *Ind. Eng. Chem. Res.* 38 (1999) 2548–2556.
- [16] S. Sitthisa, W. An, D.E. Resasco, *J. Catal.* 284 (2011) 90–101.
- [17] J. Wu, Y. Shen, C. Liu, H. Wang, C. Geng, Z. Zhang, *Catal. Commun.* 6 (2005) 633–637.
- [18] B.M. Nagaraja, A.H. Padmasri, B.D. Raju, K.S. Rama Rao, *Int. J. Hydrogen Energy* 36 (2011) 3417–3425.
- [19] H. Li, S. Zhang, H. Luo, *Mater. Lett.* 58 (2004) 2741–2746.
- [20] H. Li, H. Luo, S. Zhang, W. Dai, M. Qiao, *J. Mol. Catal. A: Chem.* 203 (2003) 267–275.
- [21] A.B. Merlo, V. Vetere, J.F. Ruggera, M.L. Casella, *Catal. Commun.* 10 (2009) 1665–1669.
- [22] D. Zhao, J. Feng, Q. Huo, N. Melosh, G.H. Fredrickson, B.F. Chmelka, G.D. Stucky, *Science* 279 (1998) 548–552.
- [23] E.P. Barrett, L.J. Joyner, P.P. Halenda, *J. Am. Chem. Soc.* 73 (1951) 373–380.
- [24] M.J. Campos Molina, R. Mariscal, M. Ojeda, M. López-Granados, *Bioresour. Technol.* 126 (2012) 321–327.
- [25] K.L. Deutscher, B.H. Shanks, *J. Catal.* 285 (2012) 235–241.
- [26] G.E. Walrafen, S.R. Samanta, *J. Chem. Phys.* 69 (1978) 493–495.
- [27] W.L. Dai, Q. Sun, J.F. Deng, D. Wu, Y.H. Sun, *Appl. Surf. Sci.* 177 (2001) 172–179.
- [28] D.E. Resasco, S. Sitthisa, J. Faria, T. Prasomriri, M.P. Ruiz, *Furfurals as chemical platform for biofuels production*, in: D. Kubíčka, I. Kubíčková (Eds.), Chapter in *Heterogeneous Catalysis in Biomass to Chemicals and Fuels*, 2012, pp. 155–188.
- [29] D. Liu, D. Zemlyanov, T. Wu, R.J. Lobo-Lapidus, J.A. Dumesic, J.T. Miller, C.L. Marshall, *J. Catal.* 299 (2013) 336–345.